



Optimal Design of a Passive SMA Damper to Control Multi-modal Stay Cable Vibrations

Selsebil Soltane¹ · Othman Ben Mekki¹ · Sami Montassar¹

Received: 5 March 2022 / Revised: 11 July 2022 / Accepted: 12 July 2022 / Published online: 4 August 2022
© Krishtel eMaging Solutions Private Limited 2022

Abstract

Purpose This paper investigates the vibration control of a stay cable using passive superelastic shape memory alloys (SMA) damper.

Methods The control of one vibration mode of a stay cable by optimized SMA damper parameters attached transversely to the cable is considered. A parametric study on two parameters, specifically, cross-sectional area and length of the damper, is conducted numerically.

Results Results show that optimized SMA damper can achieve significant damping improvement. The considered damper exhibits superior control performance over Magnetorheological damper for the target mode. However, designing the damper for a specific mode leads to vibrating other modes, revealing that optimized SMA damper is unable to provide sufficient supplemental modal damping to the stay cable. To achieve coupled multi-modal control an optimization criterion was developed through an analytical and numerical approaches.

Conclusion The optimization results indicate that the SMA damper is potential to reach a significant control performance, mitigating simultaneously the vibration of three coupled modes which looks promising for practical applications.

Keywords Shape memory alloys · Passive damper · Stayed cable vibrations · multi-modal control

Introduction

The rapid progress of the span of cable stayed bridges increases the susceptibility to exhibit large amplitudes vibration under environmental excitations, such as wind [4, 15], rain wind [4, 15, 33, 37] and parametric excitation [8, 46, 52], given that this structures are flexible and have low inherent damping [53]. Vibration can lead to breakdown stay cable connections, damage corrosion protection systems resulting on the fatigue failure of the integrity of bridge. The mitigation of the dynamic response of stay cable using mechanical active, semi active and passive dampers was widely investigated to prevent premature damage in

stay cable and improved safety and serviceability of bridges [3, 8, 19–21, 35]. Since they provide a significant damping force and present an easy replacement, mechanical dampers are applied in full-scale to medium and long span bridges [7, 54]. The frequency of vibrations induced by the rain wind is mainly between 1 Hz and 3 Hz according to a full scale measurements [31]. This range of frequency covers a number of modes for long stay cables which it is not so far perspicuous how to identify the target mode for damping. Hence, if the damper is designed for optimal performance in a specific mode can lead cable vibration of other modes [23, 29, 47]. Therefore, multi-mode cable vibration control is an important issue for development of cable stayed bridges. Many investigations have been conducted to develop the control of multi-mode cable vibration. Susumpow and Fujino [12] proposed an active control of multi-modal cable vibrations by axial support motion. Wang et al. [50] developed a new active control algorithm for optimal design of viscous dampers to reach multi-modal cable vibration control. The used method provides a high level damping to all concerned modes. Semi-active cable multi-modal vibration control using magnetorheological (MR) damper has been

✉ Selsebil Soltane
salsabil.soltane@gmail.com

Othman Ben Mekki
othman.benmekki@enit.utm.tn

Sami Montassar
sami.montassar@enit.rnu.tn

¹ Ecole Nationale d'Ingénieurs de Tunis, Université de Tunis El Manar, LGC, BP 37, Le Belvédère, 1002 Tunis, Tunisia

investigated by studies [9, 16, 32]. MR damper showed an effectiveness to provide damping for multi-mode vibration. Nevertheless, this strategy requires a power alimentation and real-time detection of vibrations which making it less recommended in practice. In recent studies, the focus is placed on performance of using passive mechanism to enhance the control several modes. The effectiveness of inerter dampers was further evaluated through the comparison with the viscous dampers in [42]. Inerter dampers was better performing than conventional viscous dampers for one mode, providing relatively limited additional damping ratios for other vibration modes. A full scale cable experiments have been carried out in [26, 27] to validate the effect of inertial dampers. Chen et al [6], studied through a parallel arrangement of a Negative stiffness mechanism and a viscous damper the control of a multi-mode cable vibration. The numerical study considering a real cable of Sutong Bridge revealed that the negative stiffness mechanism improves damping effects of all cable modes equally. Following experimental studies, [43, 55] demonstrated the performance of negative stiffness devices. Damping performance dependence of modes frequency was investigated through field tests using viscous and viscoelastic dampers [5]. Observations showed that, for a precisely range of frequency, the two aforementioned dampers provide comparable modal damping for all the tested cable modes. However, in higher modes the damping provided by the viscous damper decreases considerably. In addition, when cables vibrate in modes with frequency higher than 3.0 Hz the performance of the viscous damper has been greatly reduced. The material SMA (shape memory alloys) is smart and functional which provide interesting proprieties not present in traditionally material including large damping capacity, self-centering ability, high fatigue and corrosion strength [2, 17, 40, 45]. The smart material has the capability of undergoing large inelastic deformations and of recovering their shape by releasing applied loads without residual strain [22]. This unique propriety, known as superelasticity, results from the phase transformation separating the two crystallographic structures of the SMA: austenite and martensite. Once the critical stress is reached, a phase transformation of the austenite towards the martensite is caused, the strain of this transformation is added to the elastic strain; once the critical stress of the inverse transformation is reached, the austenitic transformation begins to take place without residual strain [49]. Consequently, the curve stress–strain is a hysteresis through the whole loading–unloading process. It presents the energy dissipation capacity and reflects the conspicuous damping property of the SMA [36, 38].

The number of studies focusing on the feasibility of using SMA as passive energy dissipation system with special emphasis on dynamic control of cable-stayed bridges has grown in the past decade and is still growing. [10] investigated through a campaign of laboratory tests the feasibility

of a hybrid control strategy by combining an open loop actuation and wrapped SMA for cable vibration mitigation. Experimental results shown on [11] confirm that the hybrid strategy promising vibration mitigation capabilities when the motion was essentially dominated by the first in-plane mode. Taking 1:60 model of the Runyang cable-stayed bridge (in Jiangsu, China) as a test platform, [13] carried out experimentations on vibration control of a stay cable with SMA damper. Results show that the SMA damper installed in plane of the cable can mitigate 50% of the free vibration. Through two sets of laboratory scale experiments realized on stayed cable, [48] report that SMA damper reduces drastically the oscillation amplitude (between 25% and 50%). The experimental results presented by [24] show that the Nickel–Titanium SMA wires permit an effective reduction of the oscillations time and their amplitudes by increasing the damping ratio.

In addition to experimental studies, many analytical approaches have been proposed. The study developed by [25] stated that the superelastic SMA damper can mitigate the cable's vibration in both cases; at its first mode or at its first few modes. The responses of a stay cable model on a cable-stayed bridge model with/without one SMA damper are numerically investigated by [28]. The study evaluates the additional equivalent modal damping ratio when the combined stay cable/SMA damper system vibrates with a single mode. [39] focused on the effect of temperature under the influence of loading. Showing that the ambient temperature has its marked effect on the superelasticity and shape memory behaviors, SMA damper made of the Ni–Ti wire can effectively quashes the stay cable vibration. A comparison between linear quadratic regulator LQR active control and passive SMA damper for controlling the cable in-plane vibration under excitations has been developed in [56]. The study reveals that the optimal control effect of the SMA damper is approached to the LQR active control effect. Other researchers have paid attention to control seismic response of cable-stayed bridges using SMA devices [14, 41].

This study highlights the performance of superelastic SMA damping device to mitigate multi-modal stay cable vibration, since large amplitude vibrations tend to be dominated by a single mode or the first modes as reported by [4, 30, 33]. The damper used is passive and must not need supervision. The paper is divided into four parts. The first part presents vibration equations of a stayed cable-SMA system specifying different hypothesis adopted in problem linearization. The second part contains an outline of the optimization method based on an energy balance used to achieve optimal damping for the first mode of vibration. The potential of SMA damper to mitigate transverse vibration stay cable belongs Rades-La Goulette cable stayed bridge is then evaluated. The case study showed that the optimal size of the SMA damper for the first mode is insufficient for control

other modes. Taking into consideration coupled modes, the third part focuses on development of an optimization method based on Irvine criterion. The last part centers on the demonstration of the effectiveness of the optimal multi-mode design of the SMA damper to control all concerned modes.

Governing Equations for a Small Sag Cable

Consider a cable suspended between two supports A and B of different heights subjected to its self-weight (cable with a sag profile). The cable is assumed to have a uniform cross-sectional area A_c along its length L and constituted by an isotropic linearly elastic material with young’s modulus E_c . The A–B line is inclined of an angle θ with respect to the horizontal. The strained static profile of the cable is spanned by the curvilinear co-ordinate s with $s = 0$ at A. The cable configuration is described in Fig. 1.

By setting the Cartesian co-ordinate system (A, x, y) , where the y axis is perpendicular to the x axis taken along the cable’s chord, the partial differential equations governing dynamic equilibrium of sagged stay cable can be written as (including the effect of SMA damper):

$$\frac{\partial}{\partial s} \left[(T + \tau) \left(\frac{dx}{ds} + \frac{\partial u}{\partial s} \right) \right] + F_{e,x}(x, t) = m_c \left[\frac{\partial^2 u}{\partial t^2} + g \sin(\theta) \right] \tag{1}$$

$$\begin{aligned} \frac{\partial}{\partial s} \left[(T + \tau) \left(\frac{dy}{ds} + \frac{\partial v}{\partial s} \right) \right] + F_{e,y}(x, t) - \sum_{i=1}^m F_{d,i}(t) \delta(x - x_d) \\ = m_c \left[\frac{\partial^2 v}{\partial t^2} - g \cos(\theta) \right] \end{aligned} \tag{2}$$

$$\frac{\partial}{\partial s} \left[(T + \tau) \frac{dw}{ds} \right] + F_{e,w}(x, t) = m_c \frac{\partial^2 w}{\partial t^2} \tag{3}$$

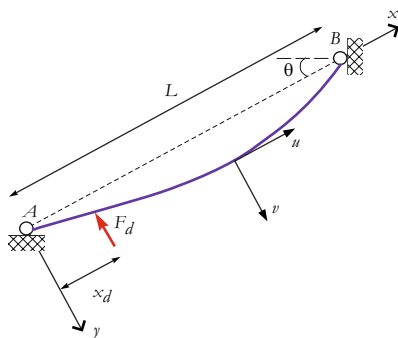


Fig. 1 Inclined cable with an attached damper

T denotes the static stay cable tension’s, τ is the additional dynamic cable tension, m_c is the mass of the cable per unit length, g is the acceleration of gravity, δ is the Dirac’s delta function, while u, v and w are the cable dynamic displacement components in the x, y and z directions, respectively; $F_{e,x}, F_{e,y}$ and $F_{e,z}$ are distributed external dynamic loading per unit length in the x, y and z directions, respectively.

The cable is subjected to a transverse concentrated force F_d generated by the SMA device attached at the location x_d from the support A in the x direction. Then, using the non-linear relationship between the dynamic cable tension and dynamic deformation:

$$\tau^D = E_c A_c \epsilon^D \tag{4}$$

The Green–Lagrange deformation is as follows:

$$\epsilon^D = \frac{\partial(u)}{\partial x} + \frac{dy}{dx} \frac{\partial v}{\partial x} + \frac{1}{2} \left[\left(\frac{\partial u}{\partial x} \right)^2 + \left(\frac{\partial v}{\partial x} \right)^2 + \left(\frac{\partial w}{\partial x} \right)^2 \right] \tag{5}$$

The aforementioned non-linear equations are simplified enforcing the following assumptions:(i) the transversal fundamental frequency of the cable is smaller than its longitudinal fundamental frequency; (ii) the cable vibrates only in the xy -plane and its motion in the x -direction is negligibly small; (iii) the static profile of the cable can be approximated to a parabola; (iv) sag length ratio is sufficiently small with respect to unit. These assumptions have been adopted in several studies (See [28, 32, 34, 44, 51] for more details). The free response of the stay cable is considered in this study, because excitations induced by wind lead to initial impulses; then the structure vibrates freely according to its natural vibration modes. The internal damping of the cable is not considered, since stay cables have very extremely low levels of inherent structural damping, typically on the order of a fraction of one per cent as indicated by several bibliographical references and full-scale tests [24].

Cable transverse free vibration, taking into account the control action with the use of a SMA damper, is governed by the following partial differential equation:

$$\begin{aligned} m_c \frac{\partial^2 v}{\partial t^2} - T \frac{\partial^2 v}{\partial x^2} + \frac{E_c A_c}{L} \left(\frac{m_c g \cos \theta}{T} \right)^2 \int_0^L v(x, t) dx \\ = - \sum_{i=1}^m F_{d,i}(t) \delta(x - x_d) \end{aligned} \tag{6}$$

The transverse deflection can be approximated using a finite modal superposition of the form:

$$v(x, t) = \sum_{i=1}^n \alpha_i(t) \phi_i(x) \tag{7}$$

where $\alpha_i(t)$ are non-dimensional modal participation factors and $\phi_i(x)$ are a set of modal shape functions, satisfying the geometric boundary conditions at the cable’s ends A and B:

$$\phi_i(0) = \phi_i(L) = 0 \tag{8}$$

To compute the damping and responses of the cable with the SMA damper, we assume sinusoidal shape functions:

$$\phi_i(x) = \sin\left(\frac{i\pi x}{L}\right) \tag{9}$$

Substituting (7) into the equation of motion (6), and using a standard Galerkin approach under the assumptions of small deflections and of linear elastic constitutive behavior results in (without external load) :

$$\sum_{i=1}^n \left[m_c \ddot{\alpha}_i(t) \int_0^L \phi_i(x) \phi_j(x) dx - T \alpha_i(t) \int_0^L \phi_i''(x) \phi_j(x) dx + \lambda^2 \alpha_i(t) \int_0^L \left(\phi_j(x) \int_0^L \phi_i(x) dx \right) dx \right] = - \int_0^L \sum_m^n F_{d,i}(t) \delta(x - x_d) dx \tag{10}$$

where

$$\lambda^2 = \frac{E_c A_c}{L} \left(\frac{m_c g \cos\theta}{T} \right)^2 \tag{11}$$

Considering only the first mode of vibration, Eq. 10 reduces to

$$m_1 \ddot{\alpha}_1(t) + (k_1 + \lambda^2 m_1) \alpha_1(t) = -F_d(t) \phi_1(x_d) \tag{12}$$

where

$$\begin{cases} m_1 = m_c \int_0^L \phi_1(x) \phi_1(x) dx = m_c \frac{L}{2} \\ k_1 = T \int_0^L \frac{d\phi_1}{dx} \frac{d\phi_1}{dx} dx = \frac{T\pi^2}{2L} \\ \phi_1(x_d) = \sin\left(\frac{\pi x_d}{L}\right) \end{cases}$$

Control of the First Vibration Mode with an Attached SMA Damper

To describe the superelastic behavior of the SMA damper, we consider a one dimensional model proposed by [1]. This model presents a shape memory alloy based damper, which exploits the superelasticity of nickel–titanium alloys (Ni–Ti) wires for energy dissipation. It takes into account one scalar internal variable ζ_s , designating the martensite fraction and consider the different elastic proprieties between the two crystallographic phases of the SMA (austenite and martensite).

Table 1 Material parameters of the element SMA

E [MPa]	σ_s^{AS} [MPa]	σ_f^{AS} [MPa]	σ_s^{SA} [MPa]	σ_f^{SA} [MPa]
50000	500	600	250	200

The numerical simulations of the constitutive equations of the model led to the curve stress strain reported in Fig. 2 considering the following properties of the element SMA presented in Table 1.

The observed curve is formed by two parts. The first consists of loading. It contains an elastic deformation from zero to σ_s^{AS} , where the elastic strain is assumed to be linearly related to the stress: $\sigma = E\epsilon^e$ with E is the elastic modulus’s austenite and ϵ^e is the elastic strain. Then, there is conversion of the austenite into martensite oriented from σ_s^{AS} to σ_f^{AS} . When the transformation is complete, there is again an elastic transformation but the Young modulus used is of the martensite. For the unloading case, the steps are the same but in reverse and the stresses used are those of martensite. As a result one hysteresis loop is formed by a closed stress strain curve in the whole loading unloading process. This hysteresis loop describes the energy dissipation ability of the SMA damper and indicates the conspicuous damper property of the SMA materials.

To investigate the performance of the SMA damper, using the model described above, on the mitigation of a stay cable first mode vibration, we proceed with solving the equation of motion (12) of the combined stay cable/SMA damper system. The device was installed on the cable at location $x_d = 0.1L$ from the left end. Since the SMA damper force cannot be decoupled due to its hysteretic performance, a nonlinear property occurs in the combined stay cable/SMA damper system. Thus, a Newmark numerical method programmed in MATLAB is developed to compute the dynamic response of the cable. The considered stay cable used to carry out this investigation is the longest cable (S16) in Rades-La Goulette cable-stayed bridge in Tunisia. The geometrical and material properties of the cable (S16) are summarized in Table 2.

It is seen from Fig. 3 that the SMA damper accomplishes a significant reduction of the first mode response, thanks to hysteretic performance, as compared to the case without the damper. Dissipating the energy coming from the motion of the stay cable, the SMA damper can effectively enhance the damping capacity of the cable. It can be also observed that when the SMA is installed the vibration amplitude is reduced very quickly. However, it can be noted from this simulation that the SMA damper is not able to control the small vibration, because the SMA deformation is smaller than 1%. In this zone, the SMA

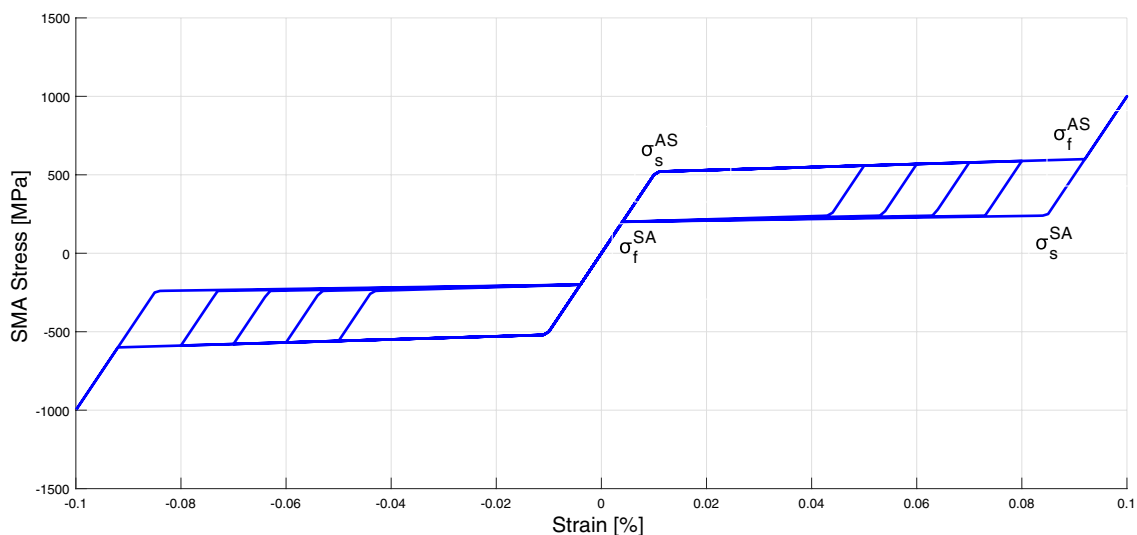


Fig. 2 Behavior and hysteresis of the one-dimensional model

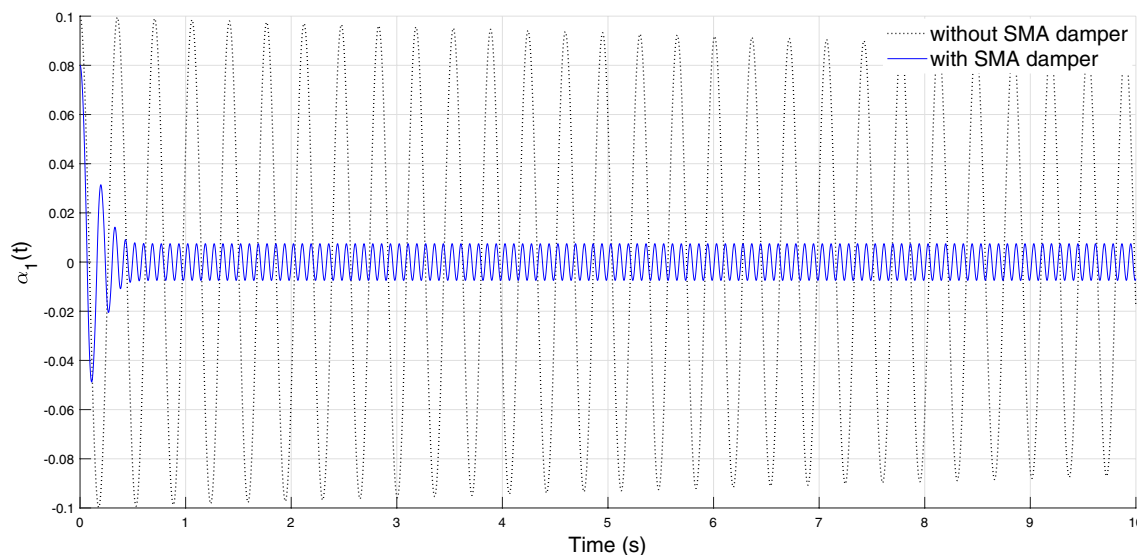


Fig. 3 First mode control with the SMA damper

Table 2 Geometrical and mechanical design properties of the stay cable (S16) of the Rades-La Goulette cable-stayed bridge

L [m]	θ [°]	T [kN]	E_c [GPa]	A_c [cm ²]	m_c [kg/m]
55.4	16.5	4313.5	190	55.5	44

has purely an elastic behavior and the hysteresis is not yet built. Nevertheless, in practice, this is not a real disadvantage, since one focuses on the large vibrations for cable-stayed bridges [34].

Optimal SMA Damper Size for Control the First Vibration Mode

In this study, we address high energy dissipation and complete deformation recovery ability as well provided by the SMA damper model. To determine the parameters leading to a maximum damping capacity, reference is made to a criterion developed in [34], which is based on the energy balance. The optimal parameters of the device in free vibration are selected in a way to maximize the force generated by the SMA damper which is expressed as follows:

$$F_d(t) = E\pi R_{SMA}^2 \left(\frac{v(x_d, t)}{L_{SMA}} - \zeta_s \epsilon_L \text{sign}(\epsilon) \right) \tag{13}$$

In which $v(x_d, t)$ denotes the cable transverse displacement at the attached point x_d , R_{SMA} is the damper wire radius, L_{SMA} represents the length of the SMA device, ζ_s is a scalar internal variable representing the martensite fraction and ϵ_L is the maximum residual strain, issue from additive decomposition of the total strain ϵ :

$$\epsilon = \epsilon^e + \epsilon_L \zeta_s \text{sgn}(\sigma) \tag{14}$$

where ϵ^e is the elastic strain.

According to (13), the damper capacity is strongly related to the SMA parameters (length and wire diameter) as well as its attached point. The position leading to a maximum force generated by the actuator is 0.5 L as shown in Fig. 4. However, it is wise to choose for practical reasons a location as close as possible to the deck side anchorage. The considered location is $x_d = 0.1 L$ from the support A in the x direction.

It's clear that the maximum damper force increases with the increase of the wire diameter and the decrease of the length of the device. To approve this numerically, we proceed first by fixing the length at $L_{SMA} = 300$ mm and varying the damper radius R_{SMA} as 2 mm, 4 mm and 10 mm, then the radius is fixed at 2 mm and the length was ranged. The choice takes into account the objectives cited above, searching for a high energy dissipation and complete deformation recovery ability and avoiding the displacement to be limited by passing solely through the original point. The decay responses of the first mode in the followed 15 s for different sectional areas are plotted for comparison in Fig. 5. It shows that the damping of the stay cable transverse vibration

increases when the damper diameter increases; Decreasing the length of the SMA damper, the amplitude of the cable transverse vibration decreases accompanied by an increase in the surface of the hysteresis loop, as shown in Fig. 6. This numerical results confirm the analytical deduction drawn from Eq. (13). Hence, for a damper located at 10% of cable length from the left anchorage, the optimum SMA damper parameters set for control the first mode vibration are $P1$: $L_{SMA} = 300$ mm and $R_{SMA} = 10$ mm.

Then, a numerical investigation which seeks to compare the performance of the optimal SMA damper size with a magnetorheological (MR) damper on the vibration mitigation of the considered cable is carried out. The idea of comparing the two devices amounts to the fact that the MR damper is filled with smart material (MR fluid) and also is able to reproduce hysterical behavior. An hysteretic regularized Bingham model (HRB) proposed and developed in [44] is used to describe the force velocity response of the MR device. The damping force defined for every piston velocity $v_d \in [-v_m, v_m]$ by

$$F_d^{HRB}(t) - F_0 = \begin{cases} C_v(v_d - v_h) + F_y \left[1 - \exp\left(-\text{sgn}(v_d - v_h) \frac{v_d - v_h}{v_0}\right) \right] \text{sgn}(v_d - v_h) & \text{for } v_d < 0 \\ C_v(v_d + v_h) + F_y \left[1 - \exp\left(-\text{sgn}(v_d + v_h) \frac{v_d + v_h}{v_0}\right) \right] \text{sgn}(v_d + v_h) & \text{for } v_d > 0 \end{cases} \tag{15}$$

where v_0 denotes the regularization parameter, which has a velocity dimension and controls the exponential growth of the damping force, v_h is a scale factor having the dimension of a velocity which defines the width of the hysteresis loop and v_m denotes the maximum reached velocity of the damper piston, v_d is the piston velocity, F_0 is the offset in

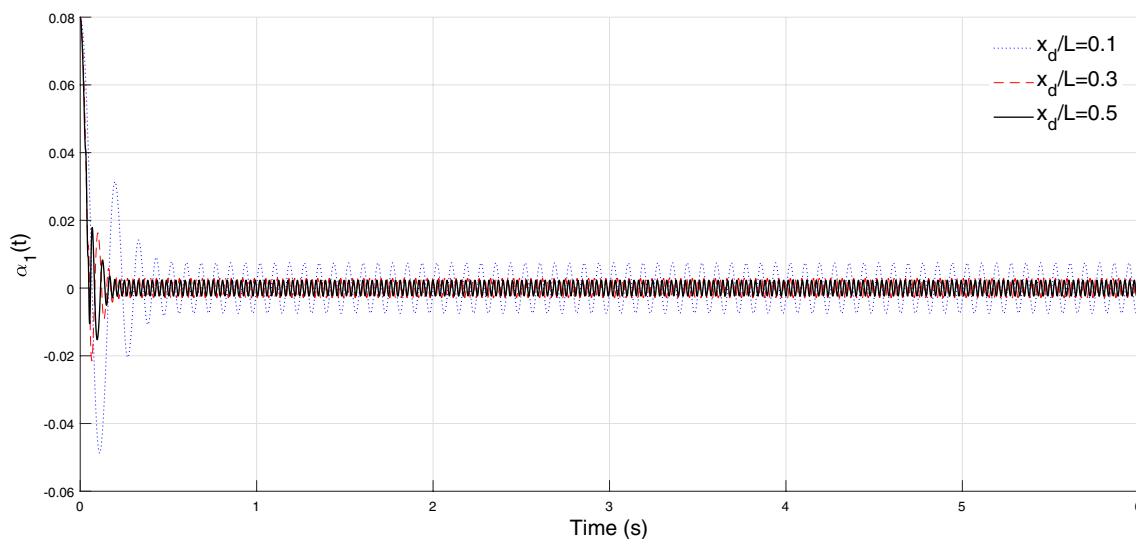


Fig. 4 Position effect of the attached SMA damper on the cable dynamic response

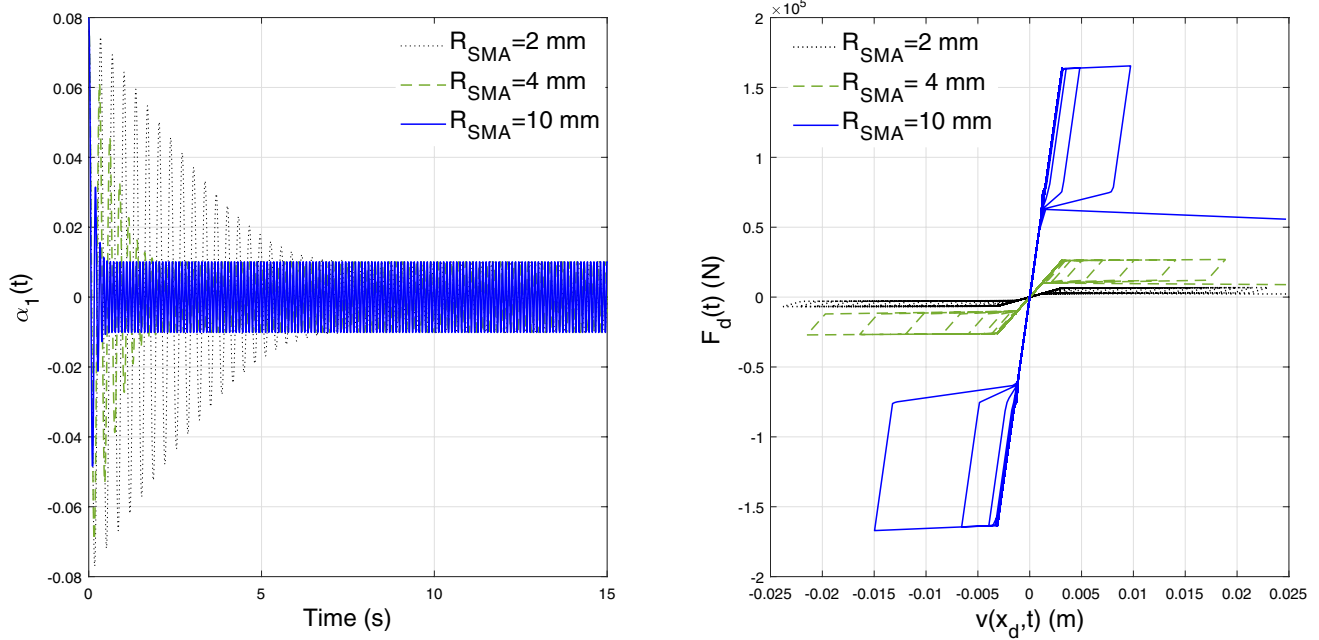


Fig. 5 Diameter effect of the attached SMA damper on the cable dynamic response— $L_{SMA} = 300$ mm

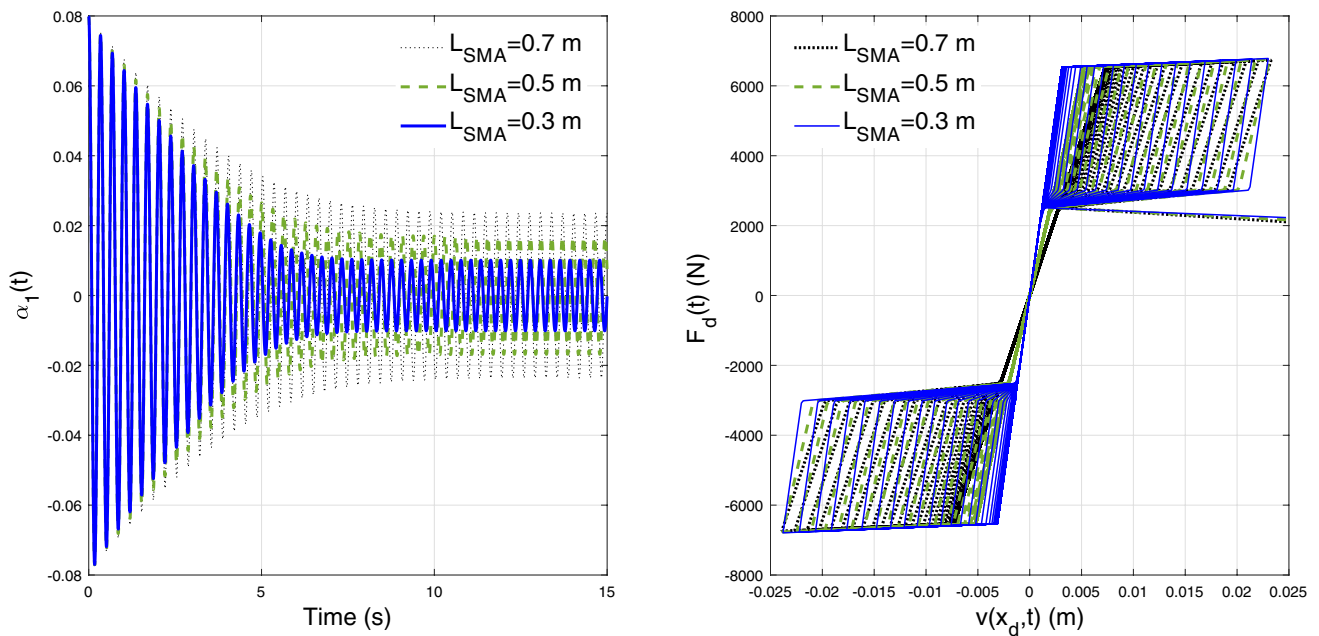


Fig. 6 Length effect of the attached SMA damper on the cable dynamic response— $R_{SMA} = 2$ mm

the damping force due to the presence of the accumulator, F_y denotes the frictional force related to the yield stress of the MR fluid (generally depending on the applied magnetic field) and C_v the damping coefficient. The latter is defined as the slope of the damping force versus the piston velocity and is related to the plastic viscosity of the MR fluid.

The obtained hysteresis loop depicted in Fig. 7 is composed of an upper curve relating to the force variation with respect to the decreasing velocities, and a lower curve

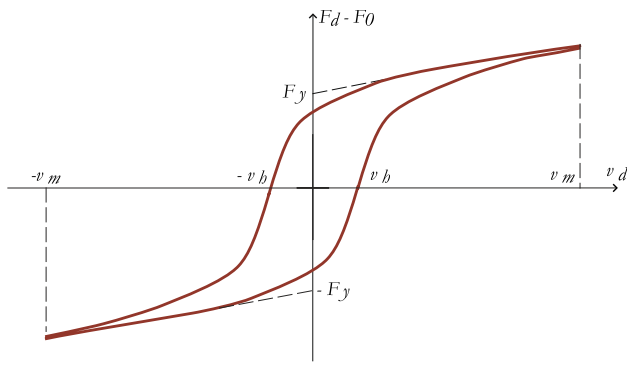


Fig. 7 Hysteretic regularized Bingham model (HRB)

corresponding to the force variation with increasing velocities. The six parameters F_0 , F_y , C_v , v_0 , v_h and v_m of the HRB model are identified by fitting the model predictions with reported experimental data (see [44]).

The MR damper used operates with step by step power supply. To switch from one input current to another, the device requires a control law, as shown in Fig. 8. We point out that the value of F_y is sensitive to the change of the electrical current supplied to the damper. However, we use the MR damper for a single step current, that of the maximum input current (2A) which leads to a passive consideration of the damper configuration.

Fig. 8 MR damper at various input currents

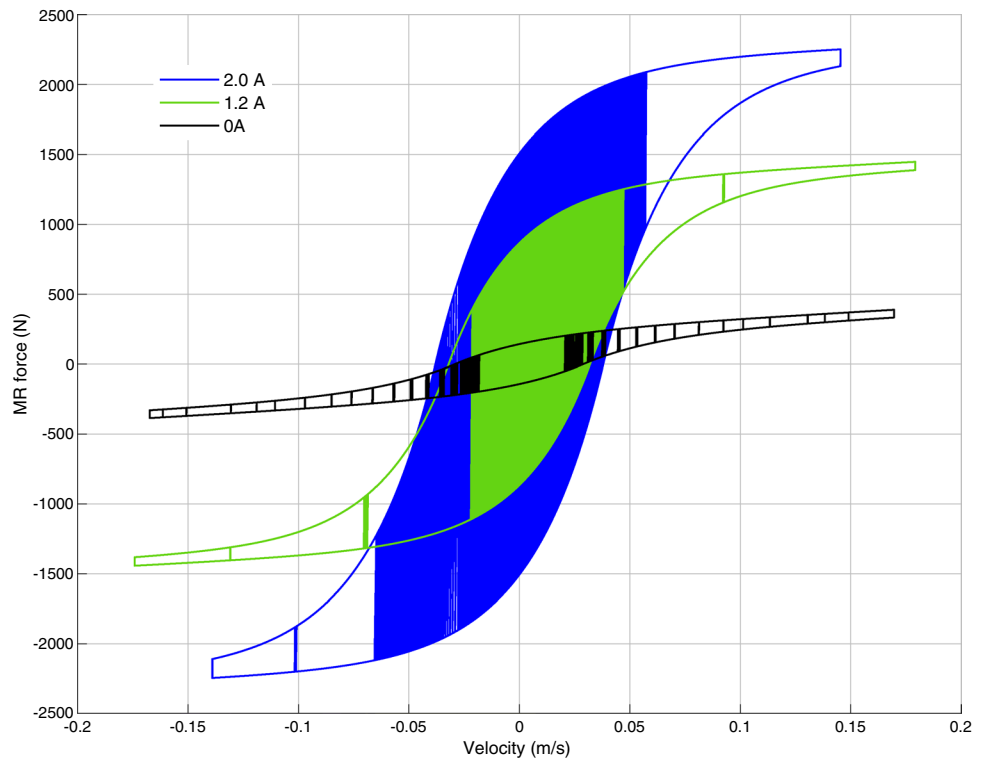


Figure 9 left outlines the vibratory response of cable controlled by MR damper described by HRB model as well as the standard Bingham model. It can be observed from Fig. 9 right the force evolutions computed by considering the HRB model and the Bingham model. It is worth noting that the cable vibration is damped more effectively when using the HRB model.

Figure 10 compares the modal contributions of the first vibration mode $\alpha_1(t)$ controlled with MR damper considering Bingham model and HRB model as well as the optimized SMA damper. Modal contributions have been obtained by solving Eq. 12. According to Fig. 10, it can be observed that the largest vibration response using the optimized SMA damper model decay speed than the one obtained using MR damper for both cases. Thus, through these results, we highlight a better performance of a passive designed SMA absorber compared to the MR absorber. These findings are important given that MR damper needs an external power supply which making it less recommended in practice.

Optimal SMA Damper Size for Control Coupled Modes

Governing Equations for Coupled System

Considering the equation of motion (10) and the sinusoidal modal shape given in (9), the elements in the Eq. (10) are calculated as follows:

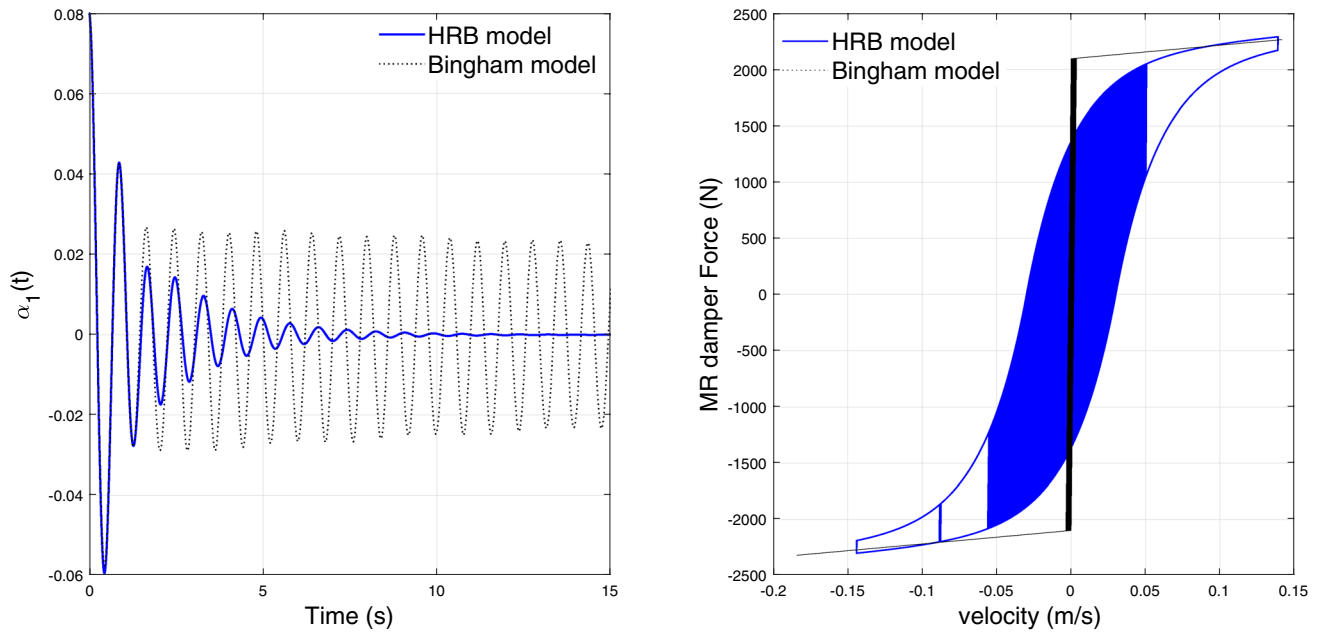


Fig. 9 Control of the first stay cable free vibration: comparison between the HRB model and the Bingham model (current 2A)

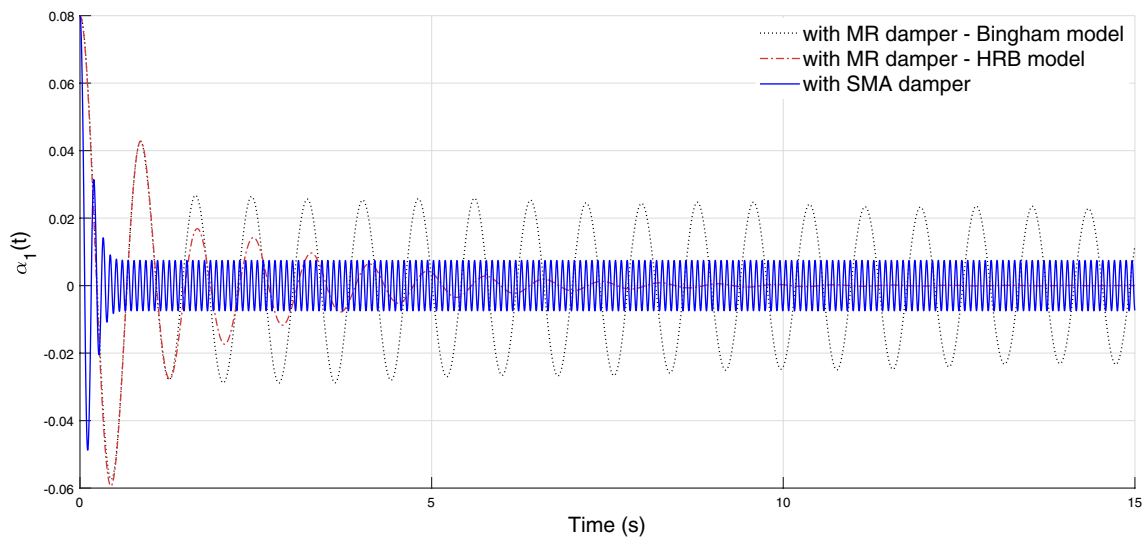


Fig. 10 Control of the first stay cable free vibration: comparison between the optimal SMA damper size $P1$ and the MR damper described with both models HRB and Bingham (current 2A)

$$\int_0^L \phi_i(x)\phi_j(x)dx = \begin{cases} L/2 & \text{if } i = j \\ 0 & \text{if } i \neq j \end{cases} \tag{16}$$

$$\int_0^L \phi_i''(x)\phi_j(x)dx = \begin{cases} -\frac{(i\pi)^2}{2L} & \text{if } i = j \\ 0 & \text{if } i \neq j \end{cases} \tag{17}$$

$$\int_0^L \left(\phi_j(x) \int_0^L \phi_i(x)dx \right) dx = \begin{cases} \frac{L^2}{(i\pi)^2}(\cos(i\pi) - 1)^2 & \text{if } i = j \\ \frac{(L)^2}{ij(\pi)^2}[\cos(j\pi)\cos(i\pi) - \cos(j\pi) - \cos(i\pi) + 1] & \text{if } i \neq j \end{cases} \tag{18}$$

The equations of the system (18) take the form:

$$\frac{(L)^2}{ij(\pi)^2}[\cos(j\pi)\cos(i\pi) - \cos(j\pi) - \cos(i\pi) + 1] = \begin{cases} 0 & \text{if } i \text{ pair and } j \text{ pair} \\ 0 & \text{if } i \text{ pair and } j \text{ impar} \\ \frac{4(L)^2}{ij(\pi)^2} & \text{if } i \text{ impar and } j \text{ impar} \end{cases} \tag{19}$$

$$\frac{L^2}{(i\pi)^2}(\cos(i\pi) - 1)^2 = \begin{cases} 0 & \text{if } i \text{ pair} \\ \frac{4(L)^2}{i\pi^2} & \text{if } i \text{ impar} \end{cases} \tag{20}$$

Considering the first three mode of vibration and substituting Eqs. (16)–(18) into Eq. (10), the non-dimensional modal participation factors projected, respectively, on the first, second and third mode are found to be

$$\begin{cases} m_c \frac{L}{2} \ddot{\alpha}_1(t) + \left(\frac{\pi^2 T}{2L} + \frac{4\lambda^2 L^2}{\pi^2} \right) \alpha_1(t) + \frac{4\lambda^2 L^2}{3\pi^2} \alpha_3(t) = -F_d(t)\phi_1(x_d) \\ m_c \frac{L}{2} \ddot{\alpha}_2(t) + \frac{4\pi^2 T}{2L} \alpha_2(t) = -F_d(t)\phi_2(x_d) \\ m_c \frac{L}{2} \ddot{\alpha}_3(t) + \left(\frac{9\pi^2 T}{2L} + \frac{4\lambda^2 L^2}{9\pi^2} \right) \alpha_3(t) + \frac{4\lambda^2 L^2}{3\pi^2} \alpha_1(t) = -F_d(t)\phi_3(x_d) \end{cases} \tag{21}$$

Written the previous equations in matrix form:

$$[\tilde{\mathbf{M}}][\ddot{\boldsymbol{\alpha}}] + [\tilde{\mathbf{K}}][\boldsymbol{\alpha}] = -[\tilde{\mathbf{F}}_d] \tag{22}$$

where

$$\tilde{\mathbf{M}} = \begin{pmatrix} m_c \frac{L}{2} & 0 & 0 \\ 0 & m_c \frac{L}{2} & 0 \\ 0 & 0 & m_c \frac{L}{2} \end{pmatrix}$$

is the mass matrix,

$$\tilde{\mathbf{K}} = \begin{pmatrix} T \frac{\pi^2}{2L} + \frac{4\lambda^2 L^2}{\pi^2} & 0 & \frac{4\lambda^2 L^2}{3\pi^2} \\ 0 & 4T \frac{\pi^2}{2L} & 0 \\ \frac{4\lambda^2 L^2}{3\pi^2} & 0 & 9T \frac{\pi^2}{2L} + \frac{4\lambda^2 L^2}{\pi^2} \end{pmatrix} \text{ is the stiffness}$$

matrix and

$$\tilde{\mathbf{F}}_d = \left[F_d \sin\left(\frac{\pi x_d}{L}\right) \quad F_d \sin\left(\frac{2\pi x_d}{L}\right) \quad F_d \sin\left(\frac{3\pi x_d}{L}\right) \right]^t \tag{23}$$

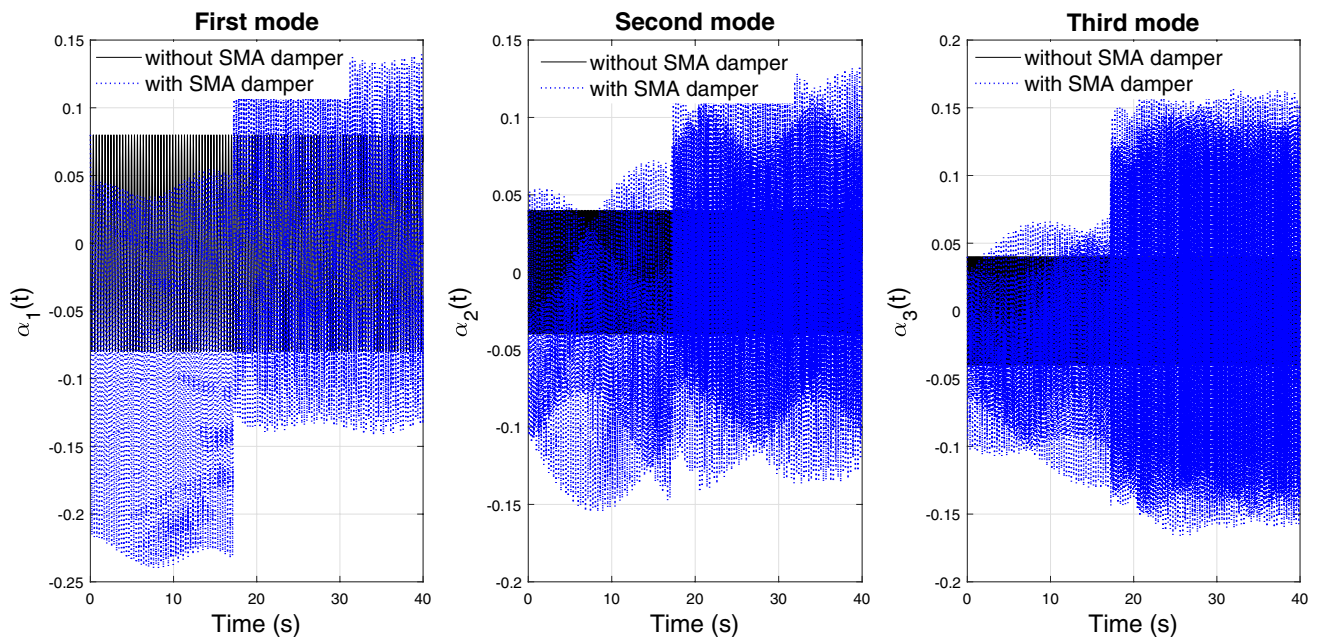


Fig. 11 Comparison between non-controlled modes and controlled modes with SMA damper using parameters set P1

is the force vector. It is useful to observe that the antisymmetric modes of vibration of the transversal dynamical equations (22) are coupled.

Control of the First Three Coupled Modes with the SMA Damper Optimized for a Single Mode

To analyze the effect of optimized SMA damper parameters $P1$ used to control the first mode of the transverse cable dynamic response, the non-dimensional modal participation factors for the three modes of the stay cable are obtained by solving (22) and considering that the SMA damper is incorporated as previously considered at $x_d = 0.1 L$.

Figure 11 illustrates the evolution of the first three modes coupled transverse free vibration, where the cable is equipped with the SMA actuator superimposed with the non-controlled modes. It's observed that the SMA damper is unable to control the three modes as well as the case of decoupling modes, even worse the presence of the SMA damper leads to an enormous increase in the vibration amplitude for the three modes considered. This result imposes the use of other optimization settings for a multi-modal control.

Optimization Criterion to Control Multiple Modes

The optimization criterion considered here is based on the calculation of an aerodynamic instability coefficient known in the literature by the Scruton number S_c that quantifies the additional damping to the cable. According to Irvine [18], a cable is aerodynamically stable, especially if he is excited by the wind or spouse wind / rain phenomenon, though its Scruton number is above a given threshold value $S_0 = 10$ [18, 50]. This number is expressed as

$$S_c = \frac{m_c \xi}{\rho D^2} \tag{24}$$

where ρ is the air density, D is the cable diameter and ξ is the equivalent damping coefficient that depends on the geometrical parameters of the actuator. Thus, an optimization criterion is formulated as follows:

$$\max_{S_c > S_0} \xi(R_{SMA}, L_{SMA}) \tag{25}$$

The calculation of equivalent damping coefficient requires the determination of the force provided by the SMA damper. It is described by a non-linear hysteresis loop, as shown in Fig. 12. The damping force is expressed on different parts of the hysteresis.

$$F_d(t) = \begin{cases} k_1 v(x_d, t) & \text{on the parts } (oab, oa'b') \\ (k_1 - k_2)v_{db} \operatorname{sgn}(v(x_d, t)) + k_2 v(x_d, t) & \text{on the parts } (bc, b'c') \\ (k_1 - k_2)(v_{da} - v_{dc} \operatorname{sgn}(v(x_d, t))) + k_1 v(x_d, t) & \text{on the parts } (cd, c'd') \\ (k_1 - k_2)v_{da} \operatorname{sgn}(v(x_d, t)) + k_2 v(x_d, t) & \text{on the parts } (da, d'a') \end{cases} \tag{26}$$

where sgn is the sign function; k_1 et k_2 are the respective slopes of the segments ab and bc ; v_{da} and F_{da} are the displacement and the damper force developed at point a ; v_{db} et F_{dy} are the displacement and the damper force developed at point b ; v_{dc} et F_{dc} are the maximal displacement and the damper force developed at point c . The damping coefficient ξ is given by [25]

$$\xi = \frac{\Delta E_{di}}{4\pi(E_{ssi} + E_{sci})} \tag{27}$$

where ΔE_{di} is twice the area of the parallelogram $abcd$ shown in Fig. 12, E_{ssi} is the deformation energy of the system cable/ SMA damper associated with the appropriate vibration mode and E_{sci} means the double surface of the trapezium $oabcv_{dc}$ shown in Fig. 12. ΔE_{di} , E_{ssi} et E_{sci} are formed as follows:

$$E_{ssi} = k_1 v_{db}^2 + k_1 [\alpha v_{dc} + (2 - \alpha)v_{db}](v_{dc} - v_{db}) \tag{28}$$

$$\Delta E_{di} = k_1 v_{db}(1 - \beta)(1 - \alpha)(v_{dc} - v_{db}) \tag{29}$$

$$E_{sci} = \frac{T \pi^2 i^2 v_{dc}^2}{kL \sin^2(i\pi x_d/L)} \tag{30}$$

where $\beta = F_{da}/F_{dy}$, $\alpha = k_1/k_2$, $k = k_1/T$.

The criterion (25) allows to take into account the multi-modal effect given that the force F_d depends on SMA geometric parameters and also on the displacement $v(x_d, t)$ of the cable at the point x_d as indicated in Eq. 13. Since

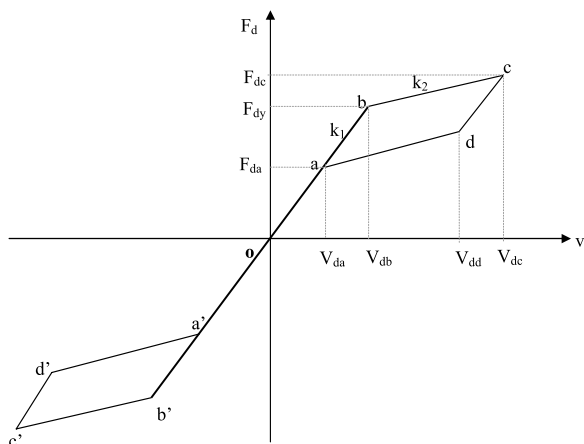


Fig. 12 Hysteresis loop produced by a SMA damper

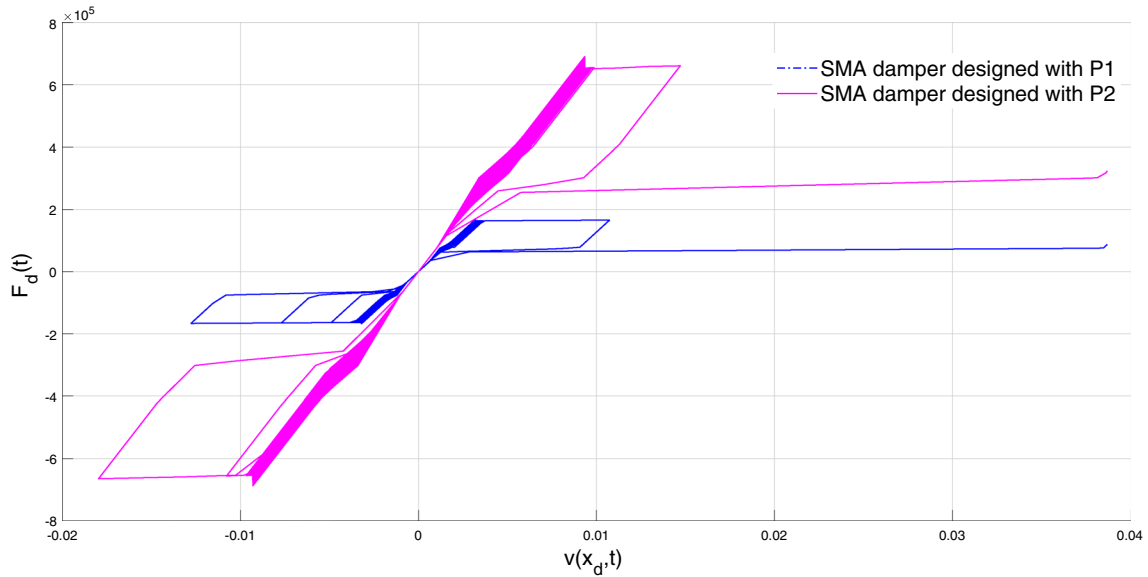


Fig. 13 Damping force for both parameter sets P1 and P2

displacement depends on all evoked modes (according to 7), the area of the hysteresis is indirectly dependent on the three modes.

Multi-modal Control Using Optimally Designed SMA Damper

The numerical resolution of the optimization criterion shown in (25) was developed to determine the optimal size

for multi-modal control (R_{SMA} and L_{SMA}). Simulations are based on the mathematical bisection method (Dichotomy). The optimization constraints satisfy: The considered R_{SMA} and L_{SMA} should be positive values and the length of the damper must be greater than the practical length (20 cm). The non-construction of hysteresis was the stop test. The optimized parameters obtained are : $R_{SMA} = 20$ mm and $L_{SMA} = 850$ mm, which will be noted in the following by P2.

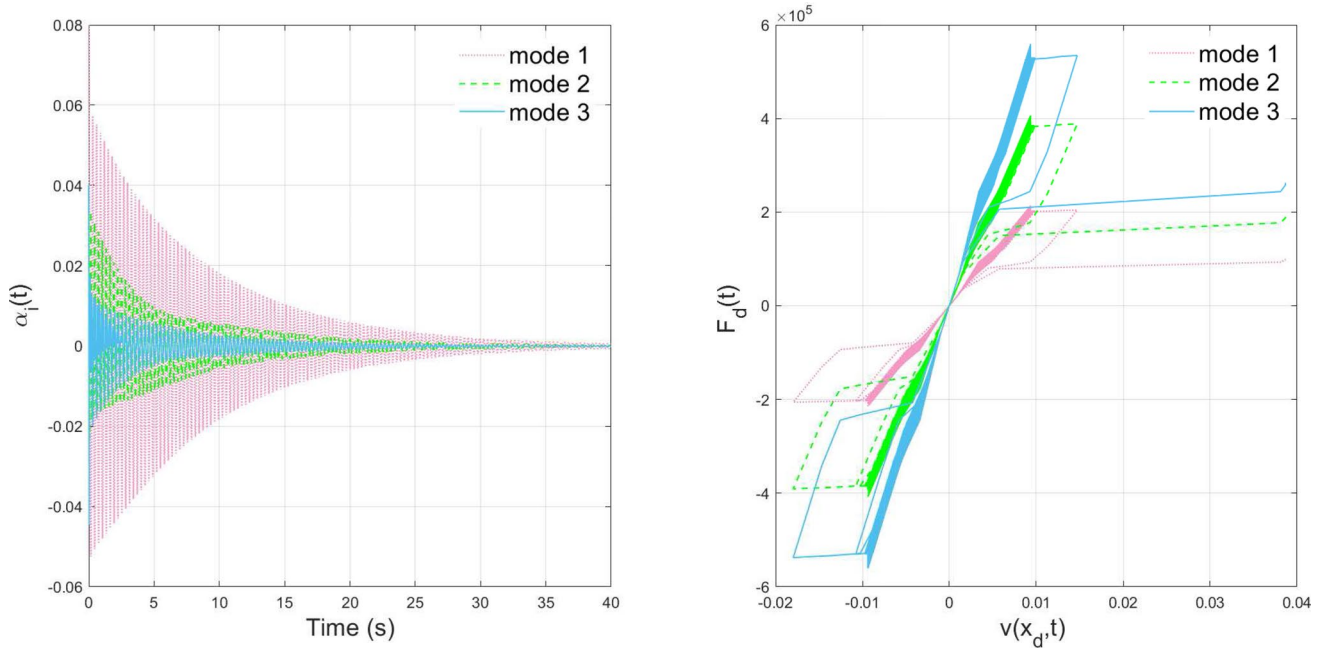


Fig. 14 Dynamic response of coupled three modes using the parameter sets P2

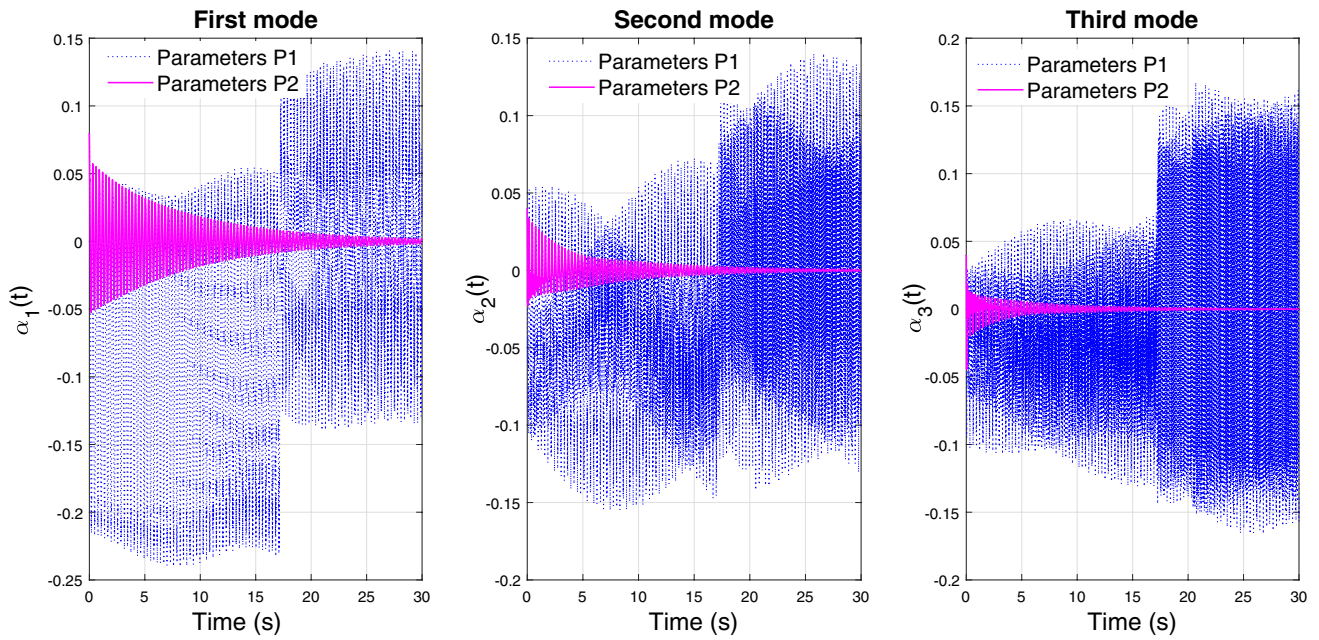


Fig. 15 Comparison between the performances of the SMA damper using the two parameter sets P1 and P2

The hysteresis curve of the total force provided by the SMA damper for both parameter sets *P1* and *P2* is shown in Fig. 13. Figure 14 presents the dynamic responses of the first three modes and the damping force produced for each mode considering parameter sets *P2*. The corresponding damping ratios are $\xi_1 = 0.458\%$, $\xi_2 = 1.7\%$,

$\xi_3 = 2.4\%$. Those associated with parameter sets *P1* are: $\xi_1 = 0.0042\%$, $\xi_2 = 0.015\%$, $\xi_3 = 0.034\%$.

Figure 15 shows the evolution of the first three modal participation of the stay cable (S16) using specific parameter *P2* to control coupled modes. These curves are compared with

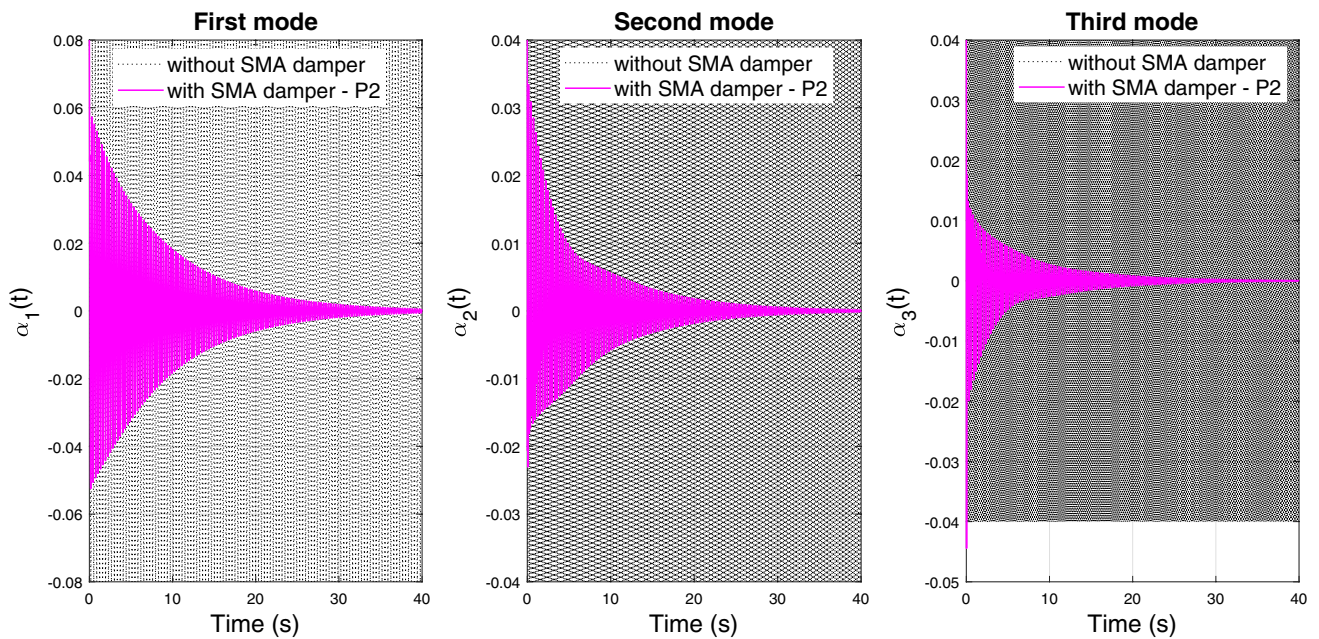


Fig. 16 Comparison between non-controlled and controlled three modes with SMA damper using parameter sets P2

those corresponding to parameter $P1$ optimized for the first mode. It follows from the comparison that the implementation of parameter sets $P2$ results in a much better damping than parameter sets $P1$ optimized for a single mode.

In addition, it mounted in Fig. 16 that optimized settings for multi-modal control $P2$ lead to a simultaneous control of the first three modes. These results are explained by the fact that the formulated optimization criterion (25) is not satisfied by considering the parameter sets $P1$, since the Scruton numbers obtained for each mode are: $S_{c1} = 0.21$, $S_{c2} = 0.76$, $S_{c3} = 1.74$. It turns out that when the damper size is optimized only for the first mode, the Scruton numbers are not enough for suppressing multi-mode vibration which much be greater than 10. However, the corresponding Scruton numbers using parameter sets $P2$ are: $S_{c1} = 23.31$, $S_{c2} = 86.53$, $S_{c3} = 122.17$. Thus leading to a spectacular reduction in the amplitudes of all concerned modes.

Conclusions

The purpose of this work is to demonstrate the effectiveness of a passive SMA damper with superelastic properties to control coupled multi-mode vibrations. The following conclusions are reported:

- Numerical simulations carried on the longest cable in the Rades-La Goulette cable-stayed bridge show the capability of SMA devise to reduce strongly the first vibration mode thanks to its excellent propriety of energy dissipation.
 - The capacity of SMA damper is closely linked to its geometric parameters. To achieve high energy dissipation, the damper size is optimized for the concerned mode through a parametric study.
 - The damping performance of the optimally designed SMA damper is numerically investigated in comparison with a magnetorheological damper. The passive designed SMA absorber is able to provide supplemental modal damping compared to MR absorber. These findings are important given that MR damper operates with a step by step power supply which making it less recommended in practice.
 - Optimized parameters for a single mode are insufficient to mitigate simultaneously three coupled modes of vibration.
- An optimization criterion is analytically formulated aiming at a multi-modal control. The parameters optimized result in a high level damping to the concerned modes. The numerical simulations demonstrate that the passive SMA damper shows an efficiency to control coupled multi-modal vibrations of the stay cable by its superelastic property. This result is important, since the fundamental operation of the passive dampers is generally designed to reduce only one mode of vibration.

Declaration

Conflict of interest On behalf of all authors, the corresponding author states that there is no conflict of interest.

References

1. Auricchio F, Sacco E (1997) A one-dimensional model for superelastic shape-memory alloys with different elastic properties between austenite and martensite. *Int J Non Linear Mech* 32:1101–1114
2. Auricchio F, Taylor R, Lubliner J (1996) Shape-memory alloys: macromodelling and numerical simulations of the superelastic behavior. *S Comput Methods Appl Mech Eng* 146:281–312
3. Baker GA, Johnson EA, Spencer BF Jr (1999) Modeling and semi active damping of stay cables. In: *Proceedings of 13th ASCE Engineering Mechanics Division Conference*, Baltimore, Maryland
4. Bosdogianni A, Olivari D (1996) Wind-and rain-induced oscillations of cables of stayed bridges. *J Wind Eng Ind Aerodyn* 64:171–185
5. Chen L, Sun L, Xu Y, Di F, Xu Y, Wang L (2020) A comparative study of multi-mode cable vibration control using viscous and viscoelastic dampers through field tests on the sutong bridge. *Eng Struct* 224:111–224
6. Chen L, Nagarajaiah S, Sun L (2021) A unified analysis of negative stiffness dampers and inerter-based absorbers for multi-mode cable vibration control. *J Sound Vib* 494:115814
7. Chen Z, Wang X, Ko Y, Ni Y, Spencer B, Yang G (2003) MR damping system on dongting lake cable-stayed bridge. *J Smart Struct Mater Int Soc Opt Photon*, pp 229–235
8. da Costa PA, Martins J, Brance F, Lilien JL (1996) Oscillations of bridge stay cables induced by periodic motions of deck and/or towers. *J Eng Mech* 7:613–622
9. Duan Y, Ni Y, Ko J (2004) Theoretical and experimental studies on semi-active feedback control of cable vibration using MR

- dampers. In: Proc. SPIE. SPIE-International Society for Optical Engineering, Bellingham 5391:543–554
10. Faravelli L, Fuggini C, Ubertini F (2009) Toward a hybrid control solution for cable dynamics: theoretical prediction and experimental validation. *Struct Control Health Monit* 17:386–403
 11. Faravelli L, Ubertini F, Fuggini C (2011) Experimental study on hybrid control of multimodal cable vibrations. *Meccanica* 46:1073–1084
 12. Fujino Y, Warnitchai P, Pacheco B (1993) Active stiffness control of cable vibration. *J Appl Mech* 60:948–953
 13. Gong L, Xuebae D (2008) Experiments of vibration control of SMA damper-stayed cable system. *J Nanjing Univ Sci Technol* 32(6):666–671
 14. Guo A, Zhao Q, Li H (2012) Experimental study of a highway bridge with shape memory alloy restrainers focusing on the mitigation of unseating and pounding. *Earthq Eng Eng Vib* 11:195–204
 15. Hikami Y, Shiraishi N (1988) Rain wind induced vibrations of cables in cable stayed bridges. *J Wind Eng Ind Aerodyn* 64:171–185
 16. Huang H, Liu J, Sun L (2015) Full-scale experimental verification on the vibration control of stay cable using optimally tuned MR damper. *Smart Struct Syst* 16:1003–1021
 17. Humbeeck JV, Kustov S (2005) Active and passive damping of noise and vibrations through shape memory alloys: applications and mechanisms. *Smart Mater Struct* 14:171–185
 18. Irvine H (1992) *Cable structures*. MIT Press, Cambridge
 19. Johnson EA, Baker GA, Spencer BF Jr, Fujino Y (2000) Mitigating stay cable oscillation using semi-active damping smart structures and materials. In: *Smart System for Bridges, Structures, and Highway*, Proc. SPIE Vol. 3988, pp 207–216
 20. Johnson EA, Christenson RE, Spencer BF Jr (2003) Semi-active damping of cables with sag compute. *Aided Civ Infrastruct Eng* 18:132–146
 21. Johnson EA, Spencer BF Jr, Fujino Y (2003) Semi-active damping of stay cables: a preliminary study. In: *Proc. 7th Int. Conf. on Modal Analysis*, Florida pp 417–423
 22. Ko J, Ni Y, Chen Z, Spencer BFJR (2006) Applications of shape memory alloys in civil structures. *Eng Struct* 28:1266–1274
 23. Krenk S (2000) Vibrations of a taut cable with an external damper. *J Appl Mech* 67:772–776
 24. Diang L, Helbert G, Chirani S, Lecompte T, Pilvin P (2013) Use of shape memory alloys damper device to mitigate vibration amplitudes of bridge cables. *J. Eng Struct* 56:1547–1556
 25. Li H, Liu M, Ou J (2004) Vibration mitigation of a stay cable with one shape memory alloy damper. *Struct Control Health Monit* 11:21–36
 26. Li J, Zhu S, Shi X, Shen W (2020) Electromagnetic shunt damper for bridge cable vibration mitigation: full-scale experimental study. *Struct Eng* 146(1):04019175
 27. Li Y, Shen W, Zhu H (2019) Vibration mitigation of stay cables using electromagnetic inertial mass dampers: full-scale experiment and analysis. *Eng Struct* 200:109693
 28. Liu M, Li H, Song G, Ou J (2007) Investigation of vibration mitigation of stay cables incorporated with superelastic shape memory alloy damper. *Smart Mater Struct* 16:2202–2213
 29. Main J, Jones N (2001) Evaluation of viscous dampers for stay-cable vibration mitigation. *ASCE J Bridge Eng* 6:385–397
 30. Main J, Jones N (2002) Free vibration of taut cable with attached damper. *J Eng Mech* 128:1072–1081
 31. Main J, Jones N, Yamaguchi H (2001) Characterization of rain wind induced stay cable vibrations from full scale measurements. In: *Proceedings of the International Symposium on Cable Dynamics*, Canada, pp 235–242
 32. Maslanka M, Sapinski B, Snamina J (2007) Experimental study of vibration control of a cable with an attached MR damper. *J Theor Appl Mech* 45:893–917
 33. Matsumoto M, Daito Y, Kanamura T, Shigemura Y, Sakuma S, Ishizaki H (1998) Wind induced vibrations of cable stayed bridges. *J Wind Eng Ind Aerodyn* 74–76:1015–1027
 34. Mekki BO, Auricchio F (2011) Performance evaluation of shape-memory-alloy superelastic behavior to control a stay cable in cable-stayed bridges. *Int J Non-Linear Mech* 46:470–477
 35. Ni YQ, Ko JM, Ying ZG, Liu HJ, Chen Y (2000) Development of smart damping systems for vibration control of civil engineering structures. In: *International Conference on Engineering and Technological Sciences ICET*, pp 858–865
 36. Pan Q, Cho C (2007) The investigation of a shape memory alloy micro-damper for mems applications. *Sensors* 7:1887–1900
 37. Peil U, Dreyer O (2006) Rain-wind induced vibrations of cables in laminar and turbulent flow. *J Wind Struct* 1:83–96
 38. Pieczyska E, Gadaj S, Nowacki W, Hoshio K, Makino Y, Tobushi H (2005) Characteristics of energy storage and dissipation in tni shape memory alloy. *J Sci Technol Adv Mater* 6:889–894
 39. Rajoriya S, Mishra S (2022) Application of SMA wire in vibration mitigation of bridge stay cable: a state of the art review. *Innov Infrastruct Solut* 7(3):192
 40. Saadat S, Salichs J, Noori M, Hou Z, Davoodi H, Baron I, Suzuki Y, Masuda A (2002) An overview of vibration and seismic application of ni-ti shape memory alloy. *Smart Mater Struct* 11(2001):218–229
 41. Sharabash A, Andrawes B (2008) Seismic control of cable stayed bridges using shape memory alloy damper. In: *The 14th Word Conference on Earthquake Engineering*, Beijing, China
 42. Shi X, Zhu S (2018) Dynamic characteristics of stay cables with inerter dampers. *J Sound Vib* 423:287–305
 43. Shi X, Zhu S, Spencer B (2017) Experimental study on passive negative stiffness damper for cable vibration mitigation. *J Eng Mech* 143:04017070
 44. Soltane S, Montassar S, Ben-Mekki O, El Fatmi R (2015) A hysteretic Bingham model for MR dampers to control cable vibrations. *J Mech Mater Struct* 10:194–208
 45. Song G, Ma N, Li H (2004) Review of applications of shape memory alloys in civil structures. In: *The 9th ASCE Aerospace Division Int. Conf. on Engineering Construction and Operations in Challenging Environments*, Houston
 46. Sun B, Wang Z, Ko JM, Ni YQ (2003) Parametrically excited oscillation of stay cable and its control in cable-stayed bridges. *J Zhejiang Univ Sci* 1:13–20
 47. Tabataba H, Mehrabi A (2000) Design of mechanical viscous dampers for stay cables. *ASCE J Bridge Eng* 5:114–123
 48. Torra V, Isalgue A, August C, Carreras G, Lovey F, Terriault P, Dieng L (2011) SMA in mitigation of external loads in civil engineering: damping actions in stayed cables. *Appl Mech Mater* 82:539–544
 49. Wang R, Cho C, Kim C, Pan Q (2006) A proposed phenomenological model for shape memory alloys. *Smart Mater Struct* 15:393–400

50. Wang X, Nib Y, Ko J, Chen Z (2005) Optimal design of viscous dampers for multi-mode vibration control of bridge cables. *Eng Struct* 27:792–800
51. Wang Z, Gao H, Fan B, Chen Z (2018) Inertial mass damper for vibration control of cable with sag. *J Low Freq Noise Vib Active Control* 39(3):749–760
52. Yamaguchi H, Fujino Y (1998) Stay cable dynamics and its vibration control. In: *Proc. Int. Symp. on Advances in Bridge Aerodynamics*, Copenhagen
53. Yamaguchi H, Fujino Y (1998) Stayed cable dynamics and its vibration control. In: *Larsen and Esdahl, Bridge Aerodynamics*, Balkema, Rotterdam
54. Zhou H, Sun L (2013) Damping of stay cable with passive-on magnetorheological damper: a full scale test. *J Civ Eng* 11:154–159
55. Zhou P, Li H (2016) Modeling and control performance of a negative stiffness damper for suppressing stay cable vibrations. *Struct Control Health Monit* 23:764–782
56. Zuo X, Li A, Sun W, Sun X (2009) Optimal design of shape memory alloy damper for cable vibration control. *J Vib Control* 15:897–921

Publisher's Note Springer Nature remains neutral with regard to jurisdictional claims in published maps and institutional affiliations.

Springer Nature or its licensor holds exclusive rights to this article under a publishing agreement with the author(s) or other rightsholder(s); author self-archiving of the accepted manuscript version of this article is solely governed by the terms of such publishing agreement and applicable law.